# ARTICLE

Alexander Mogilner · George Oster

# The polymerization ratchet model explains the force-velocity relation for growing microtubules

**Abstract** The polymerization of filamentous proteins generates mechanical forces which drive many cellular processes. Dogterom and Yurke measured the force-velocity relation generated by a single microtubule. They found that the force is generally in the range predicted by the "polymerization ratchet" mechanism, but the force-velocity relationship decreased faster than that theory predicted. Here we generalize the polymerization ratchet model to take into account the "subsidy effect" that arises because a microtubule consists of 13 protofilaments. With this generalization the model fits the experimental data well. The biological implications of the polymerization ratchet model are discussed.

**Key words** Filamentous proteins · Polymerization rachet model · Microtubules · Force-velocity relationship

## Introduction

Microtubules (MTs) are linear polymers composed of asymmetric globular subunits; they are found in all eucaryotic cells (Bray 1992; Alberts et al. 1994). MTs assemble and disassemble at different rates from the "plus" (growing) and "minus" (shrinking) ends. The tubulin subunits are aligned in 13 parallel protofilaments, each composed of repeating tubulin dimers linked head to tail. MTs provide the tracks upon which protein motors transport vesicles and organelles, and they determine the polarity and directionality of motile cells. They are of paramount significance in the mitotic apparatus during mitosis. For ex-

A. Mogilner (✉)
Department of Mathematics, University of California,
Davis, CA 95616, USA
e-mail: mogilner@math.ucdavis.edu

G. Oster
Department of Molecular & Cellular Biology and College
of Natural Resources, University of California, Berkeley,
CA 94720-3112, USA

ample, MTs participate in generating the force driving chromosome movements in prometaphase (Bray 1992; Alberts et al. 1994). These forces are quite large – amounting to hundreds of piconewtons (pN) (Mitchison 1988; Inoue and Salmon 1995). Both polymerization and depolymerization at the MT's plus end are involved in the force generation mechanism (Mitchison 1988; Inoue and Salmon 1995).

Dogterom and Yurke (1997) measured the force generated by the growing MTs. In their experiments, growing fibers 30 μm in length impinged on the wall of a well in the experimental chamber and buckled. After buckling, the filaments continued to grow, but at a slower rate. These experiments indicated that growing MTs are able to generate a force exceeding the buckling load. By quantifying the shapes of the bent fibers, computing the corresponding elastic force resisting elongation, and measuring the respective rates of growth, the authors were able to compute the force-velocity relation for a growing MT for forces up to 4 pN. Their force-velocity relation could be approximated by an exponential dependence: $v \approx \exp(-f/\kappa)$, where $\kappa$ is the flexural rigidity of the MT. They concluded that the force derived from the free energy of polymerization.

Peskin et al. (1993) formulated a mechanistic theory to account for the force generated by a polymerization process when the filaments are rigid. They proposed that the addition of subunits to the end of growing filaments rectified the brownian motion of a diffusing object in front of the filament, and showed that this "ratcheting" of diffusive motion could generate sufficient force to account for a number of motile phenomena. The polymerization process produced an axial force by employing the free energy of polymerization to render unidirectional the otherwise random thermal fluctuations of the load. Their model assumed that the polymer was infinitely stiff, and so the brownian motion of the load alone created a gap sufficient for monomers to intercalate between the tip and the load. Dogterom and Yurke (1997) showed that the theory of Peskin et al. gives the right order of magnitude of the growth rate at a given load force, but quantitatively the theoretical result overestimates the experimental data. Here we demon-

strate that the polymerization ratchet model can be generalized to explain quantitatively the experimental results of Dogterom and Yurke (1996a, b).

Mogilner and Oster (1996a, b) generalized the rigid polymerization ratchet theory for rectified diffusion to the situation when the polymerizing filaments are flexible, so that their thermal fluctuations are sufficient to create a monomer-sized gap to permit polymerization. The principle result of this generalization was an expression for the effective polymerization velocity of a growing filament as a function of the load force and the effective elastic and diffusion coefficients characterizing the filament. Here we further generalize the model to describe the growth of MTs and compare our estimates with the experimental measurements.

## A model for microtubule growth

Figure 1 shows a schematic view of the MT and chamber wall. We treat the MT filament as a bundle of 13 cross-linked protofilaments which is polymerizing perpendicularly to the barrier. An elastic load force, $f$ opposes the growth of the filament. We assume that all protofilaments polymerize and depolymerize independently in the same direction. This means that MT assembly is the result of 13 independently polymerizing protofilaments.

However, the force generated by all 13 filaments is not simply the sum of the forces generated by each protofilament, for this would significantly overestimate the net force. The reason is apparent: at any instant, those protofilaments that are too close to the wall cannot polymerize very fast because the gaps between their tips and the wall are not wide enough to allow the intercalation of a tubulin dimer. Nevertheless, these protofilaments can "subsidize" the growth of the neighboring filaments which are farther from the wall by supporting a large portion of the load. Before we analyze this *subsidy effect,* we must formulate the effective rate of tip assembly.

### Effective rates of tubulin assembly onto the tip of the protofilament

Far from the wall, the assembly and disassembly of subunits onto the protofilament tips takes place with the rates $k_{on}$, $k_{off}$, respectively. Because $k_{off} \ll k_{on}$ (Drechsel et al. 1992), the effect of the load force on the net growth rate is negligible, and we can assume that the rate of disassembly is constant, and independent of the load force. Initially, we shall assume that $k_{off}=0$; later we shall use $k_{off}$ as a parameter to obtain a best fit to the data [see Discussion below, and also the discussion in Dogterom and Yurke (1997)].

If a protofilament's tip finds itself a distance $y < \delta = 8$ nm from the wall (the size of a tubulin dimer), then a dimer cannot intercalate onto the tip. In order to add a monomer a thermal fluctuation must bend the MT sufficiently to create a monomer-sized gap [bending is much easier than
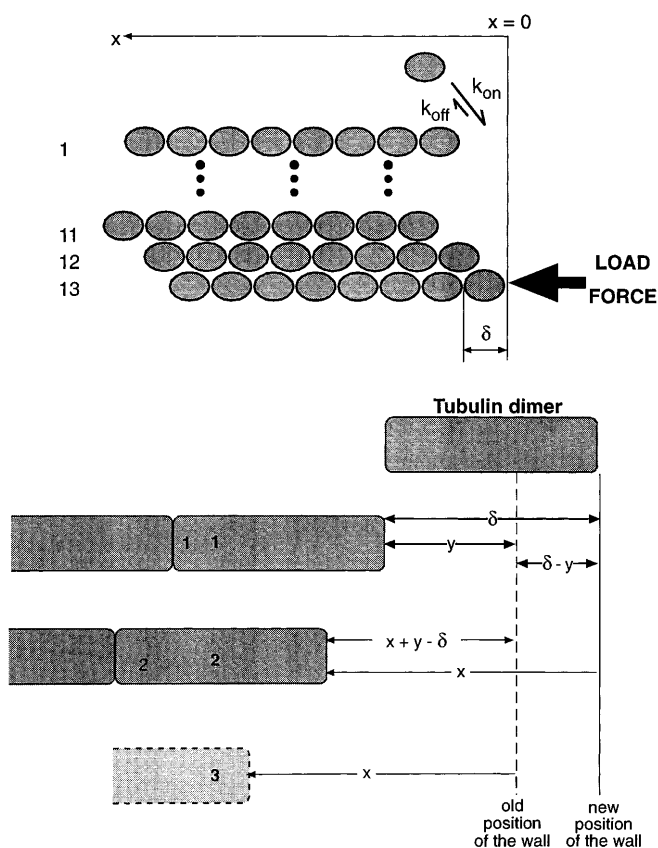


**Fig. 1** We assume that the 13 protofilaments grow independently against the elastic load force created by the MT buckling against the wall of the experimental chamber described in Dogterom and Yurke (1997). A tubulin dimer detaches from the protofilament tip at the rate $k_{off}$, assumed to be independent of the load force. The corresponding rate of dimer assembly, $k_{on}$, is conditional on the existence of a gap of size $\delta$ or greater between the tip and the wall. The changes in the density distribution of tips due to an elementary act of polymerization are shown schematically. We measure the distance, $x$, to the left from the leading tip of the fiber to a tip lagging behind. When a tubulin dimer of size $\delta$ assembles onto the tip of protofilament 1 which is initially at a distance $y < \delta$ from the leading tip, the leading tip advances to $x=(\delta-y)$. Protofilament 2 that was originally at distance $(x+y-\delta)$ from the leading tip jumps to position $x$, while protofilament 3 that was originally at a distance $x$ from the leading tip jumps farther away. These jumps are described by the integral kernels in Eqs. (2) and (3)

compression (Gittes et al. 1996)]. In Mogilner and Oster (1996a, b) we proved that if the thermal bending fluctuations are fast in comparison with the assembly process, and if the bending elastic energy is less than thermal energy, then the assembly rate, $k_{on}$, is altered by the Boltzmann factor $\exp[f(y-\delta)/k_B T]$ where $f$ is the load force, $T$ is the absolute temperature, and $k_B$ is Boltzmann constant.

This expression can be understood as follows. When bending fluctuations are rapid, the assembly process is near thermodynamic equilibrium. The work needed to increase the gap by the distance $(\delta-y)$ against the load force $f$ is $f(\delta-y)$. Then the Boltzmann factor determines the decrease in the effective rate of assembly. In Appendix A we show that these conditions are satisfied, so the effective

rate of tubulin assembly onto the protofilament's tip is given by the expression:

$$p(f, y) = k_{\text{on}} \exp[f(y-\delta)/k_{\text{B}}T] \qquad (1)$$

## Collective dynamics of the distribution of the protofilament's tips

Next, we consider $N$ protofilament tips polymerizing against the wall. We assume that the longest protofilament can support the MT against the wall. We place our coordinate system at the tip of the leading protofilament and measure positive displacements perpendicularly inward. Let $n(x, t)$ be the continuous spatial density of the filament tips. The dynamics of this density is described by the following set of deterministic equations derived in Appendix B:

$$\frac{\partial n}{\partial t} = \underbrace{k_{\text{on}}\,(n(x+\delta) - n(x))}_{\substack{\text{Appearance of tips at posi-} \\ \text{tion } x \text{ due to polymerization}}} + \underbrace{k_{\text{off}}\,(n(x-\delta) - n(x))}_{\substack{\text{Appearance of tips at posi-} \\ \text{tion } x \text{ due to depolymerization}}}$$

$$+ \underbrace{\int_0^\delta p(f, y)\, n(y)\, n(x+y-\delta)\, \mathrm{d}y}_{\substack{\text{Gain of tips at position } x \text{ due to} \\ \text{polymerization of tips at } y}}$$ (2)

$$- \underbrace{n(x) \int_0^\delta p(f, y)\, n(y)\, \mathrm{d}y}_{\substack{\text{Loss of tips at position } x \\ \text{due to polymerization at } y}}, \quad x \geq \delta$$

$$\frac{\partial n}{\partial t} = \underbrace{k_{\text{on}}\, n(x+\delta)}_{\substack{\text{Appearance of tips} \\ \text{at position } x \text{ due to} \\ \text{polymerization}}} - \underbrace{k_{\text{off}}\, n(x)}_{\substack{\text{Appearance of tips} \\ \text{at position } x \text{ due to} \\ \text{depolymerization}}}$$

$$+ \underbrace{\int_{\delta-x}^\delta p(f, y)\, n(y)\, n(x+y-\delta)\, \mathrm{d}y}_{\substack{\text{Gain of tips at position } x \text{ due to} \\ \text{polymerization of tips at position } y}}$$ (3)

$$- \underbrace{n(x) \int_0^\delta p(f, y)\, n(y)\, \mathrm{d}y}_{\substack{\text{Loss of tips at position } x \\ \text{due to polymerization at } y}}, \quad 0 \leq x < \delta$$

Equation (2) describes the situation when $x > \delta$. The first term describes the rate of change of the tip density due to the free assembly of a dimer of size $\delta$ onto a tip. The second term accounts for the corresponding process of disassembly. Equation (3) describes the situation when $(x-\delta) < 0$. The first and second terms describe assembly and disassembly, respectively, close to the leading tip. Disassembly cannot increase the concentration of the tips at $x$ because there are no tips within $x < 0$, while free assembly cannot take place too close to the wall. The integral terms are due to polymerization of those tips which are closer than $\delta$ to the leading tip (see Appendix B for detailed description and derivations).

As explained in Appendix B, the above description of the tip ensemble is continuous and deterministic, and so disregards stochastic fluctuations in the distribution of the relatively small number of the protofilaments. This approximation is very rough when the number of protofilaments $N = 13$ (the corresponding relative error cannot be estimated accurately for this complicated nonlocal nonlinear model, but in principle it can be as great as $\sim 1/\sqrt{N} \approx 25\%$). In order to obtain some reassurance that the actual error is tolerable, we performed simulations of a discrete stochastic model described in Appendix D. The results (see Fig. A 2 in Appendix D) show that the continuous deterministic model provides good qualitative description of MT growth.

The continuous model cannot be used at very small load forces. In this situation there is exactly one tip propping up the wall, while the computed density of the protofilament tips would be very small at $x = 0$. This would give a significant error at forces less than $\sim 0.5$ pN, and so we did not use the model for simulations of load forces $< 0.5$ pN. For forces less, but close to, 0.5 pN we are unable to compute the growth rates accurately. However, for forces much less than 0.5 pN, the analytical result for the growth rate $V \approx V(0) \exp[-f\delta/k_{\text{B}}T]$ is a good approximation. (This expression can be easily obtained from the fact that, with high probability, there is only one leading protofilament, while the other 12 of protofilaments are lagging behind by a distance greater than $\delta$. The free rate of growth of the advanced tip, $V(0)$, is then altered by the Boltzmann factor $\exp[-f\delta/k_{\text{B}}T]$.) Equations (2) and (3) are nonlinear integral-differential-difference equations. The nonlinearity is due to the effective interactions between the protofilament tips caused by the subsidy effect. These equations cannot be approximated by partial differential equations, because the density of tips changes significantly on the size scale of a dimer. Therefore, they must be solved numerically.

## Effective growth rate

The effective growth rate of the MT can be calculated as follows. If a tubulin dimer assembles on a protofilament tip at a distance $x$ from the leading tip, then the advance of the leading tip increases by a distance $(\delta-x)$. This happens at a rate equal to the effective polymerization rate $p(f, x)$ times the density $n(x)$, of the tips: $p(f, x) \times n(x)$. Each such polymerization contributes to the protrusion rate by $p(f, x) \times n(x) \times (\delta-x)$. Summing the corresponding rates and taking the depolymerization into account, we find the effective average protrusion velocity to be

$$V(f) = -k_{\text{off}}\,\delta + \int_0^\delta (\delta-x)\, p(f, x)\, n(x)\, \mathrm{d}x \qquad (4)$$

## Results

Equations (1)–(3) were solved numerically for values of the load force from 0.5 to 4 pN (see Appendix C). An asymptotically stable stationary distribution, $n(x)$, of the
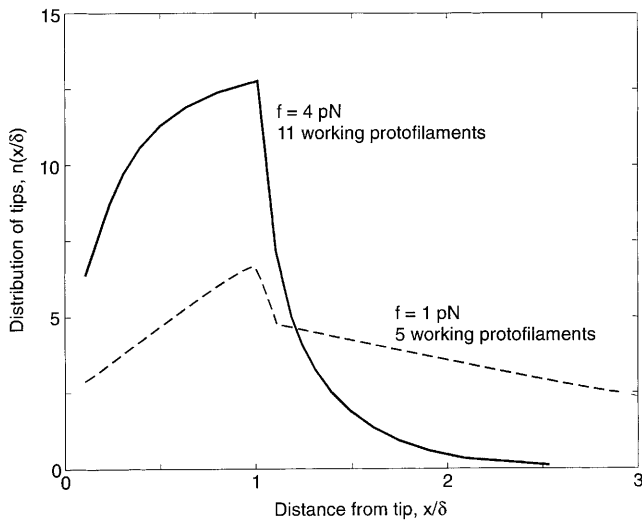
**Fig. 2** Computed stationary spatial distributions of the protofilament tips. The *dashed line* shows the number of tips as a function of the distance from the leading tip when the load force equals 1 pN. The number of "working" protofilaments consists of those closer than $\delta$ to the wall, so that their growth contributes to the protrusion force. In the dashed curve, this is approximately equal to 5. The *solid curve* shows the distribution of tips corresponding to a force of 4 pN and about 11 working protofilaments. Greater forces produce slower protrusion, so more tips polymerize closer to the wall
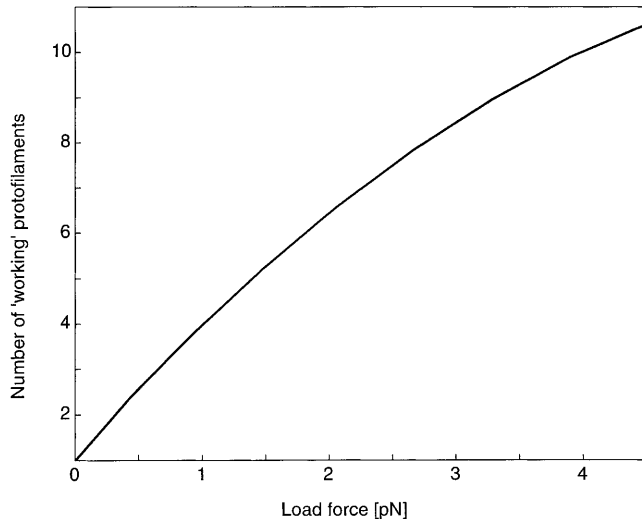


**Fig. 3** The computed number of "working" protofilaments (those whose tips are closer than the dimer size to the wall) as a function of the load

tips was reached within a few tens of the assembly time-scale. The results for load forces $f = 1$ and 4 pN are shown in Fig. 2. At distances greater than $\delta$, the density of tips decreases away from the wall because the tips grow faster than the average MT polymerization rate. At large forces, more protofilament tips catch up with the tip of the MT, and so the total number of "working protofilaments" (i.e. those within distance $\delta$ of the wall) grows with the load force. The corresponding dependence is illustrated in
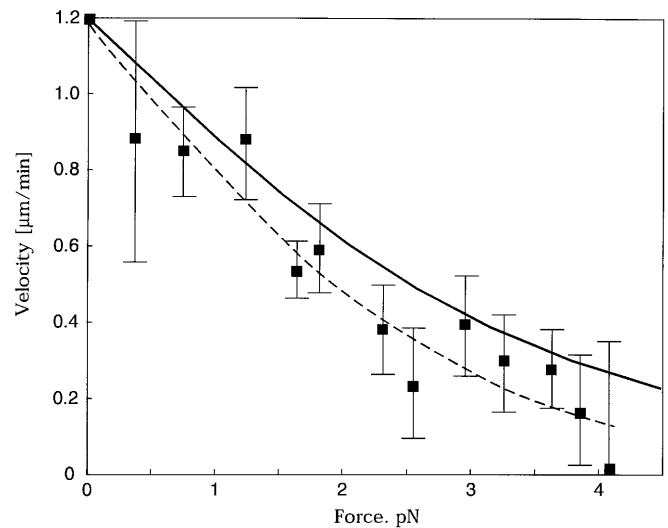


**Fig. 4** The *solid curve* shows the computed force-velocity relation for the growing MT. The solid squares with error bars are the experimental data (Dogterom and Yurke 1997). The *dashed curve* shows the best fit to the experimental data obtained using assembly and disassembly rates provided in the text

**Table 1** Parameter values

| Parameter | Value | Reference |
|---|---|---|
| $k_B T$ = thermal energy | 4.1 pN×nm | Peskin et al. (1993) |
| $\delta$ = size of tubulin dimer | 8 nm | Alberts et al. (1994) |
| $B$ = flexural rigidity of MTs | 34 pN×μm | Dogterom and Yurke (1997) |
| $D$ = effective diffusion coefficient of MTs | 0.09 μm²/s | Computed |
| $N$ = number of protofilaments | 13 | Alberts et al. (1994) |
| $\ell$ = length of MTs | 30 μm | Dogterom and Yurke (1997) |
| $V(0) = k_{on} \delta$ = free growth rate | 1.2 μm/min | Dogterom and Yurke (1997) |
| $k_{off} \delta$ = depolymerization rate | 0 | Assumption |

Fig. 3. Thus only a subset of the protofilaments is responsible for growth, while the rest "subsidize" them against the load. This effect is largely responsible for the relatively low growth rate of microtubules.

The concentration of tips is maximum at $x = \delta$ and decreases closer to the wall (almost linearly at low load forces, and more slowly at greater forces). This is because each individual protofilament is inhibited near the wall, and so grows slower than the MT as a whole. This difference diminishes as the load force increases.

Combining the computed tip distributions, $n(x)$, at different forces and Eqs. (1) and (4) for the effective growth rate, we computed the force-velocity relation for a growing MT below the stall force (Dogterom and Yurke 1997). Since $k_{off} \ll k_{on}$, we assumed $k_{off} = 0$ (Drechsel et al. 1992) and $k_{on} = V(0)/\delta = (1.2 \text{ μm/min})/8 \text{ nm}$. The results shown in Fig. 4 are in good quantitative agreement with the experimental results of (Dogterom and Yurke 1997).

Figure 4 shows that, despite this agreement, the theoretical results still predict slightly greater values of the growth rate. Varying the value of force independent disassembly rate, $k_{off}$, we found that the theoretical force-velocity relation (dashed curve in Fig. 4) fits the experimental results best at values $k_{on} \approx (1.4$ μm/min$)/8$ nm and $k_{off} \approx (0.2$ μm/min$)/8$ nm. (Assembly/disassembly rates were chosen so that the free net polymerization rate was equal to the observed value $V(0) = 1.2$ μm/min; see the parameter values in Table 1.)

## Discussion

By extending the polymerization ratchet models (Peskin et al. 1993; Mogilner and Oster 1996a, b) to permit flexible filaments and "subsidy" by leading filaments, we have been able to construct a more complete picture of the physics of force generation by a growing polymer. The measurements of (Dogterom and Yurke 1997) were performed at load forces less than 4 pN. At such forces, growth was inhibited, but not stopped completely. Dimensional and numerical analyses of the polymerization ratchet model equations indicate that at large load forces (i.e. $f \gg (k_B T/\delta)\sqrt{N} = 1.85$ pN) all protofilament tips are within a distance $\delta$ from the wall, and their distribution asymptotically approaches a constant (cf. Fig. 2): $n(x) \approx N/\delta$ at $0 < x < \delta$, and $n(x) \approx$ at $x > \delta$. Using this result and Eq. (4) for the MT growth rate, we obtain an approximate expression for the growth at large load forces:

$$V(f) \approx \delta \left( k_{on} \, N \left( \frac{k_B T}{f \, \delta} \right)^2 - k_{off} \right) \tag{5}$$

At $f = 4$ pN the analytical result (5) (corresponding to the best fit) gives the value of $V(f) \approx 0.1$ μm/min, very close to the numerical result.

Note that the asymptotic velocity of protrusion decreases inversely as the load force, not exponentially, as predicted by models which ignore the subsidy effect. (This difference might be hard to detect experimentally.) Solving Eq. (5) for $V(f) = 0$, we obtain the approximate expression for the stall force:

$$f_{stall} \approx \frac{k_B T}{\delta} \sqrt{\frac{k_{on}}{k_{off}}} \sqrt{N} \tag{6}$$

Using the estimates $k_{on} = V(0)/\delta = (1.4$ μm/min$)/8$ nm and $k_{off} \approx w/\delta = (0.2$ μm/min$)/8$ nm from the best fit, we estimate the force generated by the polymerization of one MT fiber $\approx 5$ pN. Note that this is the same order of magnitude as the stall force of kinesin (Block 1995). The disassembly rate predicted from fitting the experimental data seems somewhat large. In Appendix D we argue that our model overestimates the growth rates at large load force. Thus, true value of the disassembly rate has to be smaller. In fact, one of the uses of Eq. (6) may be in estimating the disassembly rate if the stall force is measured.

Equation (6) gives a scaling relation for the dependence of the force on the number of the protofilaments: $f \propto N^{1/2}$. Qualitatively, this result can be understood as follows. Close to stall, a protofilament is near thermodynamic equilibrium where $f \approx k_B T/\delta$ (Hill 1987). At large load forces only some of the "working" protofilaments whose tips are in the interval $[\delta - (k_B T/f), \delta]$ can both polymerize effectively and generate force. The number of such filaments is $\sim N(k_B T/f \delta)$. In other words, the number of protofilaments that generate protrusive force is inversely proportional to the load force. The rest of the working protofilaments are not polymerizing, but are "propping" up the load and subsidizing the polymerizing force generating protofilaments. The total force can be found from the relation $f \propto N^{1/2}$. Rigorously speaking, Eqs. (5) and (6) must be used in the limit of large $N$. In our case, when $N = 13$, the condition of their validity, $f \gg 1.85$ pN, means that even very close to the stall force the results would be correct only within an order of magnitude.

Note that the assumption of additive polymerization of the protofilaments would have allowed us to use the results of Mogilner and Oster (1996a, b) and Peskin et al. (1993) directly and predict the force-velocity relation $V \approx V(0) \exp [-f \delta/N k_B T]$. This result gives the incorrect scaling relation $f \approx N$, and also predicts growth rates greater than those observed (Dogterom and Yurke 1997).

Good agreement of the theoretical results with the experimental data also indicates that there is no slow rate-limiting step in the process of dimer assembly (e.g. there is no slow chemical reaction after a dimer assembles onto a protofilament's tip that has to be completed before the polymerization can continue). In the latter case, the growth rate would be almost independent of the load force up to a critical value, after which the effective polymerization velocity would rapidly decrease as the force increases (Wang et al. 1998).

The polymerization ratchet model predicts that the growth rates and forces would be significantly lower if the fibers are short enough that filament bending requires energies comparable to thermal energy. The critical length of MT below which this effect comes into play is $L_{cr} \approx (B \delta/k_B T)^{1/2} \approx 8$ μm.

The generalized polymerization ratchet model introduced here may account for the microtubule driven deformation of liposomes observed in several experiments (Miyamoto and Hotani 1988; Miyata and Hotani 1992; Fygenson 1995). The theory also accounts for several features of filopodial protrusion (Bray 1992), where 20–30 cross-linked actin filaments polymerize against the cell membrane. In fact, the quantitative results are better in that case, because the deterministic model works better as $N$ grows. This will be described elsewhere (Mogilner and Oster, in preparation).
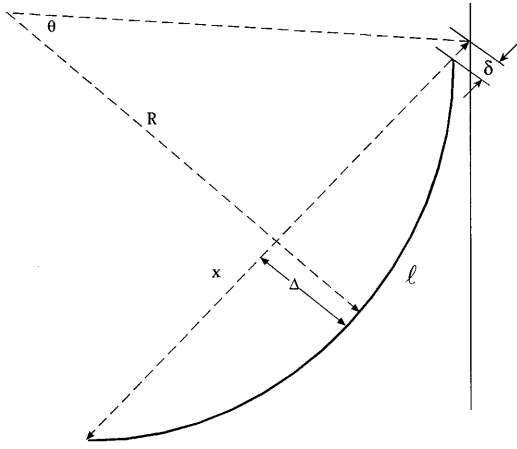
**Fig. A1** Schematic illustration of the geometry of the bent filament

---

## Appendices

### A. Thermally driven undulations are much faster than polymerization rates

Here we demonstrate that the timescale for MT fluctuations is much smaller than that for dimer assembly. First we estimate an effective diffusion coefficient (normal to the major axis) for a MT of length $\ell = 30\ \mu\text{m}$ and diameter $d = 25\ \text{nm}$ (Alberts et al. 1994). We approximate the tubule as a long prolate ellipsoid, for which the drag coefficient is $\zeta = 4\pi\eta\ell/(\ln(2\ell/d)+1/2)$ (Berg 1983). Using the viscosity of water, $\eta = 0.01\ \text{P} = 0.001\ \text{pN}\times\text{s}/\mu\text{m}^2$, $D = k_B T/\zeta \approx 0.09\ \mu\text{m}^2/\text{s}$. Beyond the buckling load, a MT can be bent to significant curvatures with a force only slightly greater than the critical buckling force (Landau and Lifshitz 1970). From the data in Dogterom and Yurke (1997) we can estimate the radius of curvature of the fiber as $R \approx 100\ \mu\text{m}$ or less. The distance between the ends of the fiber is $x \approx 2R\sin(\ell/2R) \approx \ell - (\ell^3/24R^2)$, when the tip of the MT touches the wall (see Fig. A1). When thermal bending fluctuations decrease the radius of curvature by $\delta R$, the distance between the tip of the fiber and the barrier increases by $\delta x \approx -(dx/dR)\,\delta R \approx (\ell^3/12R^3)\,\delta R$. At the same time, sidewise displacement of the fiber is $\Delta = R(1 - \cos(\ell/2R)) \approx \ell^2/8R$, which increases by $\delta\Delta \approx -(d\Delta/dR)\,\delta R \approx (\ell^2/8R^2)\,\delta R$. Then, expressing the change in the radius of curvature in terms of the distance between the tip and barrier, and substituting the result into the equation for the sidewise displacement, we obtain the following approximate relation: $\delta\Delta \approx (3R/2\ell)\,\delta x$. In order to find the characteristic sidewise displacement necessary to create a gap between the tip and the wall of size $\delta$, we substitute the values of $\delta = 8\ \text{nm}$, $\ell = 30\ \mu\text{m}$, and $R \approx 100\ \mu\text{m}$ into the last relation to find that $\delta\Delta \approx 40\ \text{nm}$ (at smaller values of $R$ the estimates become even more favorable). The corresponding timescale for the tip fluctuations is $(\delta\Delta)^2/D \approx 0.018\ \text{s}$. Compare this with the polymerization timescale: $\delta/V(0) \approx 0.4\ \text{s} \gg (\delta\Delta)^2/D$. Thus thermal fluctuations are frequent enough to permit subunits to intercalate onto polymerizing MT ends.

### B. Derivation of the continuous deterministic model

We describe the tip of the microtubule fiber by the integer state variable $N(x, t)$ that represents the number of protofilament tips at distance $x$ from the tips of the leading protofilament(s) at time $t$. Based on the helical arrangement of the protofilaments in a fiber, the size of the tubulin dimer $\delta = 8\ \text{nm}$, and the assumption about rigid cross-linking of the protofilaments in the tubule, the natural choice for the independent variable $x$ would be the set $x = \{(\delta/13)\,j\}, j = 0, 1, \dots$.

  A. The stochastic processes and corresponding changes in the state of a fiber occurring at location $x \geq \delta$ are:

1. Increase of the number of tips by one owing to the free assembly of a dimer of size $\delta$ onto a tip at location $(x+\delta)$. The corresponding rate is $k_{on}N(x+\delta)$.
2. Increase of the number of tips by one owing to the disassembly of a dimer at location $(x-\delta)$. The corresponding rate is $k_{off}N(x-\delta)$.
3. Decrease of the number of tips by one owing to the free assembly of a dimer onto a tip at location $x$. The corresponding rate is $k_{on}N(x)$.
4. Decrease of the number of tips by one owing to the disassembly of a dimer at location $x$. The corresponding rate is $k_{off}N(x)$.
5. Increase of the number of tips by $N(x+y-\delta)$, $y < \delta$, owing to polymerization of the tips at location $y < \delta$. The corresponding rate is $p(f, y)\,N(y)$. This can be understood as follows (refer to Fig. 1). Assume that a dimer assembles onto tip 1 located at position $y$ ($0 < y < \delta$). Then the leading tip (always at $x = 0$) moves a distance $(\delta - y)$. Then tip 2, located at $(x + y - \delta)$, jumps to location $x$. Note that in order to find the corresponding average change in the state $N(x)$, we must sum over all locations such that $y < \delta$. This reasoning is not completely correct at location $x = \delta$ because then the corresponding increase of the number of tips is $(N(\delta+y-\delta)-1) = (N(y)-1)$. (One of the tips from location $y$ becomes the leading one; the remaining $(N(y)-1)$ assume the new distance $\delta = y + \delta - y$ away from the leading tip.) The deterministic model derived below is rigorously valid only in the limit $N(x) \to \infty$, and then the corresponding error of relative magnitude $(1/N)$ can be neglected.
6. The decrease in the number of tips by $N(x)$ owing to polymerization of the tips which are closer than $\delta$ to the wall – and consequent change in the location of all tips relative to the new position of the most advanced tip. (Refer to Fig. 1: tip 3 at point $x$ leaves its position.) The corresponding rate is $\sum_{y<\delta} p(f, y)\,N(y)$.

  B. The stochastic processes 1, 4, and 6 and corresponding changes in the state of a fiber at location $0 < x < \delta$ (closer than the size of a dimer to the leading tip) are the same as those described above for locations $x \geq \delta$. Process 2 is absent (there is no tips at location $(x-\delta) < 0$), as well as pro-
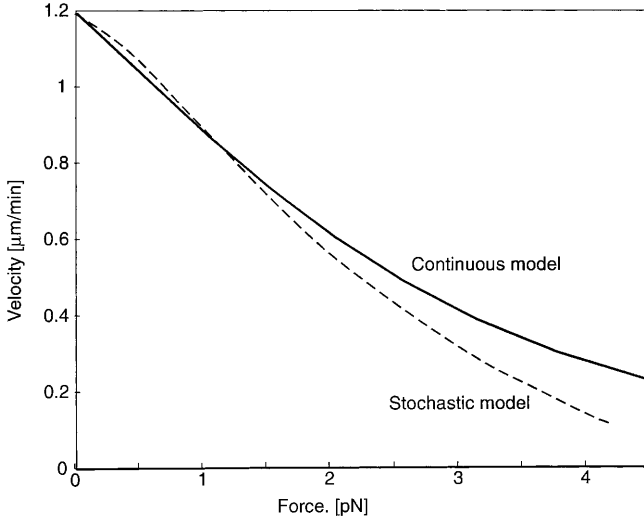
**Fig. A2** The *solid curve* shows the force-velocity relation for the growing MT computed from the continuous deterministic model. The *dashed curve* shows the average force-velocity relation obtained from the discrete stochastic model

$$\frac{\langle \Delta N(x)\rangle}{\Delta t} = k_{on}\,(N(x+\delta) - N(x)) + k_{off}\,(N(x-\delta) - N(x))$$
$$+ \sum_{y<\delta} p(f,y)\,N(y)\,N(x+y-\delta)$$
$$- N(x) \sum_{y<\delta} p(f,y)\,N(y),\quad x \geq \delta$$

$$\frac{\langle \Delta N(x)\rangle}{\Delta t} = k_{on}\,(N(x+\delta) - k_{off}\,N(x)$$
$$+ \sum_{\delta-x<y<\delta} p(f,y)\,N(y)\,N(x+y-\delta)$$
$$- N(x) \sum_{y<\delta} p(f,y)\,N(y),\quad 0 \leq x < \delta$$

In the limit of a large number of protofilaments, each exerting an infinitesimal effect on the others, the stochastic nature of the system vanishes, so the expectations on the left hand sides disappear. To get the continuous deterministic analogue of this model we scale $N(x,t)$ to a density $n(x,t) = N(x,t)/(\delta/13)$. Converting sums to integrals we thus derive the integro-differential Eqs. (2) and (3) for the spatial density $n(x,t)$. By construction, Eqs. (2) and (3) conserve the total number of tips: $N=\int_0^\infty n(x,t)\,dx=\text{const.}$

## C. Numerical solutions

Equations (2) and (3) were non-dimensionalized and solved on the interval $0<x<6\,\delta$, which was discretized into $78=6\times13$ mesh points. Uniform initial conditions and no flux boundary conditions were used. The trapezoidal rule was used to compute the integral terms. The equations were integrated with the help of the Forward Euler method using Matlab. The corresponding M-files are available on request.

## D. Simulations of discrete stochastic model

To build confidence in our deterministic continuous model, we simulated 13 tips growing stochastically according to the following rules:

1. Initial conditions were 13 tips located equidistantly with spatial increment $(\delta/13)$.
2. At each time step, $dt$, the leading tips were identified. If a tip was at a distance greater or equal than $\delta$ from the leading set, it was moved a distance $\delta$ forward with probability $k_{on}\,dt$.
3. If a tip was at a distance $y$ less than $\delta$ from the leading set, it was moved a distance $\delta$ forward with probability $k_{on}\,\exp(f(\delta-y)/k_B T)\,dt$.

The results of a 100 runs (500 time steps each) were averaged to get the average force-velocity relation shown in Fig. A2 (dashed curve). The result compares favorably with the continuous deterministic force-velocity relation (solid curve). The deterministic model underestimates the velocity at small forces and overestimates the number of

cess 3 (assembly at location $x<\delta$ shifts the whole tips distribution). When considering process 5 for tips located closer than $\delta$ to the leading tip, the following change has to be made: the summation over location $y$ has to be performed for $y > \delta-x$ (otherwise $x+y-\delta<0$, and there is no increase in the number of tips at location $x$).

C. Everything said in (B) is valid for the most advanced location $x=0$ if the following important assumptions are made:

– In the limit $N\to\infty$, where the deterministic approach is valid, the probability that there is only one tip at the leading position can be neglected. Then, at any instant, depolymerization of a tip from this position does not cause the shift of the whole distribution, because other tips at the same location remain the leading ones.
– We remarked above that when an act of assembly occurs at location $y<\delta$, then one tip from that location becomes the leading one, while the remaining $(N(y)-1)$ tips jump to a new location. However, we neglected the difference between $N(y)$ and $(N(y)-1)$ in point A.5, and to be consistent we have to neglect the corresponding increase of the number of tips by 1 with rate $\sum_{y<\delta} p(f,y)\,N(y)$ at location $x=0$. The respective correction may not be small for $N(0,t)$. Nevertheless, when we calculate the effective velocity of polymer growth, it will be expressed in terms of the convolution of the local assembly rate with distribution $N(x)$. Omitting the process described here introduces an error only of order $1/N$.

Based on this description of continuous-time stochastic process (A–C) and calculating the expected change in the number of tips at location $x$ between times $t$ and $t+\Delta t$, conditional on the entire state of the system at time $t$, we arrive at the following system of equations:

protofilaments at distances close to $\delta$ from the most advanced tip. Thus we obtain a positive error for predicted velocities at greater forces.

## References

Alberts B, Bray D, Lewis J, Raff, Roberts K, Watson J (1994) Molecular biology of the cell, 3rd edn. Garland, New York

Berg H (1983) Random walks in biology. Princeton University Press, Princeton

Block S (1995) Nanometers and piconewtons: the macromolecular mechanics of kinesin. Trends Cell Biol 5: 169–175

Bray D (1992) Cell movements. Garland, New York

Dogterom M, Yurke B (1997) Measurement of the force-velocity relation of growing microtubules. Science 278: 856–860

Drechsel DN, Hyman AA, Cobb MH, Kirschner MW (1992) Modulation of the dynamic instability of tubulin assembly by microtubule-associated protein tau. Mol Biol Cell 3: 1141–1154

Fygenson D (1995) Microtubules: the rhythm of assembly and the evolution of form. PhD Thesis, Princeton University, Princeton

Gittes F, Meyhofer E, Baek S, Howard J (1996) Directional loading of the kinesin motor molecule as it buckles a microtubule. Biophys J 70: 418–429

Hill TL (1987) Linear aggregation theory in cell biology, Springer, Berlin Heidelberg New York

Inoue S, Salmon ED (1995) Force generation by microtubule assembly/disassembly in mitosis and related movements. Mol Biol Cell 6: 1148–1163

Landau L, Lifshitz E (1970) The theory of elasticity, 2nd edn. Pergamon Press, London

Mitchison TJ (1988) Microtubule dynamics and kinetochore function in mitosis. Annu Rev Cell Biol 4: 527–549

Miyamoto H, Hotani H (1988) Polymerization of microtubules within liposomes produces morphological change of their shapes. In: Hotani H (ed) Taniguchi international symposium on dynamics of microtubules, vol 14. Taniguchi Foundation, Taniguchi, pp 220–242

Miyata H, Hotani H (1992) Morphological changes in liposomes caused by polymerization of encapsulated actin and spontaneous formation of actin bundles. Proc Natl Acad Sci USA 89: 11547–11551

Mogilner A, Oster G (1996a) Cell motility driven by actin polymerization. Biophys J 71: 3030–3045

Mogilner A, Oster G (1996b) The physics of lamellipodial protrusion. Eur Biophys J 25: 47–53

Peskin C, Odell G, Oster G (1993) Cellular motions and thermal fluctuations: the Brownian ratchet. Biophys J 65: 316–324

Wang H, Elston T, Mogilner A, Oster G (1998) Force production in RNA polymerase. Biophys J 74: 1186–1202